



AIAA 99-4806
Integrating Aeroheating and TPS Into
Conceptual RLV Design

K. Cowart
J. Olds
Georgia Institute of Technology
Atlanta, GA

9th International Space Planes and Hypersonic
Systems and Technologies Conference
and
3rd Weakly Ionized Gases Workshop
1-5 November 1999
Norfolk, VA

Integrating Aeroheating and TPS Into Conceptual RLV Design

Karl K. Cowart[†]

Dr. John R. Olds^{*}

Space Systems Design Laboratory

School of Aerospace Engineering

Georgia Institute of Technology, Atlanta, GA 30332-0150

ABSTRACT

The purpose of this study is to develop the Thermal Calculation Analysis Tool (TCAT) that will enable Aeroheating and Thermal Protection System (TPS) sizing to be an on-line, automated process. This process is described as dynamic on-line TPS sizing. It enables the assumptions made about the vehicle TPS to be updated through out the iteration process. This method is faster and more accurate than a static off-line process where the assumptions of the vehicle TPS are held constant during the vehicle design procedure. TCAT will work in conjunction with other engineering disciplines in a Design Structure Matrix (DSM). The unsteady, one dimensional heat diffusion equation was discretized, and resulted in a tridiagonal system of non-linear algebraic equations. This system was implicitly solved using the iterative Newton-Raphson technique at each time level. This technique was conducted for both steady-state and transient conditions that predicted the temperature profiles, and in-depth conduction histories for several TPS material test cases. Also, this was performed on several disparate TPS materials layered together at one time. Finally, comparative benchmark solutions of the TCAT transient analyses were conducted using the commercial software code SINDA/G. Results show that TCAT performed as predicted, and will satisfy the requirement of lowering the amount of time required to conduct TPS sizing for a reusable launch vehicle. Future work will consist of adding temperature dependent material properties to TCAT, coupling TCAT to an optimizer, and creating a web-interface that will enable cross-platform operation of TCAT.

[†] - Graduate Student, School of Aerospace Engineering,
Graduate Research Assistant, Student member AIAA.

^{*} - Assistant Professor, School of Aerospace Engineering,
Senior member AIAA.

NOMENCLATURE

DSM	design structure matrix
MDO	multidisciplinary design optimization
MMFD	modified method of feasible directions
RCC	reinforced Carbon-Carbon Composite
RLV	reusable launch vehicle
RTV	room temperature vulcanizing adhesive
SIP	strain isolator pad
SLP	sequential linear programming
SQP	sequential quadratic programming
SSDL	Space System Design Lab
STS	Space Transportation System
TCAT	Thermal Calculation Analysis Tool
TPS	thermal protection system
TPSX	Thermal Protection System Expert
TRL	technology readiness level
TUFI	toughened unit-piece fibrous insulation
UHTC	ultra high temperature ceramics

INTRODUCTION

TPS sizing calls for the selection of materials that effectively protects the space vehicle and its cargo/passengers from the severe heating environment created during reentry and ascent. After making the appropriate selection of the constituent materials of the TPS, the unit weight, acreage percentage and the thickness of each are determined.

The remainder of this paper will discuss the differences between static and dynamic TPS sizing along with the proof of concept in the development of the TCAT tool. Static TPS sizing calls for making assumptions before the design iteration process. One example can be constant a unit weight. These assumptions remain constant during the design of a vehicle. Dynamic TPS sizing allows the assumptions made apriori in the design process to be updated throughout the iteration cycle. Dynamic TPS sizing is the preferred method of the two available. This is because the ability to update the assumptions used

during the iteration process provides more confidence in the final solution. The proof of concept involves three test cases that show steady-state and transient analysis capabilities of TCAT. Along with these test cases, a transient analysis was performed on a layer of five different TPS materials. Also, benchmark solutions with a commercial Aeroheating software package, and future work considerations are presented.

STATIC OFF-LINE TPS SIZING

In many design organizations, Aeroheating is done in the conceptual design phase. Often it is an off-line static process where single point assumptions are made about TPS unit weights, thicknesses, and acre percentages. These single point assumptions are set at the beginning of the design, and are not changed throughout the convergence process. As a consequence, this means no communication occurs between the aeroheating and aerodynamics disciplines shown in the Design Structure Matrix of Figure 1.

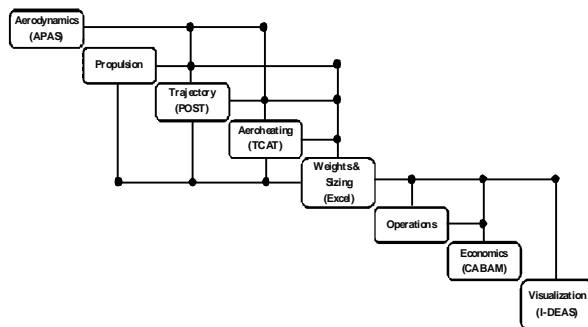


Figure 1. Design Structure Matrix (DSM).

The feedback with Aerodynamics is important because the leading edges of the vehicle could be too small, thereby creating heat loads that are too high, based on the assumed TPS. To lower the heat loads, the Aeroheating analyst desires blunt leading edges for lower heat loads. An Aerodynamicist desires sharp, small radii leading edges that minimize the drag. These two disciplines conflict with each other. Therefore, there is an optimum leading edge value that must be found so that both disciplines are satisfied. Integrated Aeroheating will help find this optimum value.

Another consequence that arises when making these off-line assumptions is that there is no interaction between the Aeroheating and Weights and

Sizing disciplines. This is similar to the situation between Aeroheating and Aerodynamics where there is an optimum value that must be reached. Here the optimum is to design a TPS structure with the minimum unit weight. If fixed assumptions are made at the beginning of the design phase, then no optimum values can be reached. Also, the assumptions made may be too conservative producing a TPS that is too thick and heavy. Or, on the other hand, the assumptions may produce a TPS that will do its job ineffectively.

Static off-line TPS sizing is a drawn-out endeavor. Several tools have to be manually run before finalized answers for the values of the thicknesses, unit weights and acre percentages are determined.

A typical static off-line TPS design procedure is as follows. The first tool run is MINIVER¹, which is an aeroheating code written by NASA. It produces center line radiation equilibrium temperature distributions, convective heating rates, and heat loads over simplified vehicle geometries. These geometries include flat plates to model wings, and swept cylinders to model leading edges. Once MINIVER has been run, the appropriate TPS material must be selected from the TPSX material database.² Figure 2 shows an example of a TPS material from the database.

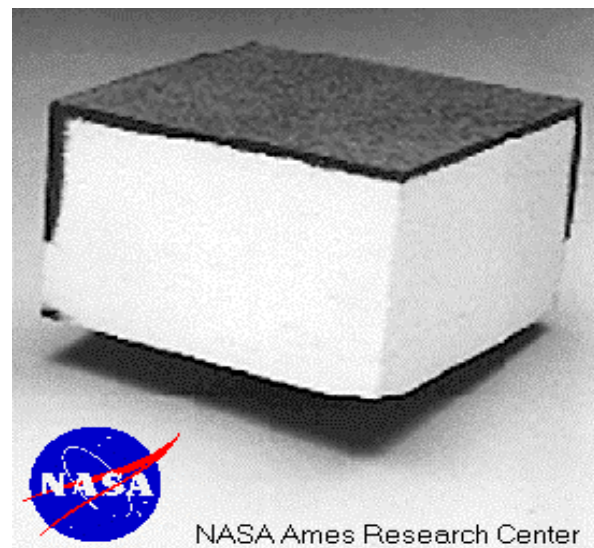


Figure 2. TUFIT Tile Composite.

After running MINIVER and obtaining the appropriate material properties list, the TPS unit weights, thicknesses, and acre percentages are determined. This process has to be conducted at several different points of interest on the vehicle, which can significantly increase the total time it takes to conduct the TPS sizing process.

There are several reasons why this process needs to be improved. First, static off-line TPS sizing may involve making faulty assumptions that may lead to non-optimal design results. Secondly, there is no coupling mechanism that allows the analysis of the in-depth conduction based on the convective heating rates obtained from MINIVER. Also, the process is too time-consuming. It might take several days, which would delay the turn-around time for a vehicle design. All these lessons call for the coupling of TPS sizing into a design oriented structure. This change will lead to dynamic on-line TPS sizing.

DYNAMIC ON-LINE TPS SIZING

The integration of TPS sizing into the DSM in the near future will enable TPS sizing to be a dynamic process. This means the sized TPS values will be revised and optimized during each iteration until the vehicle is converged. This integrated approach will involve the coupling of four tools: MINIVER, TPSX, TCAT and a numerical optimizer.

Descriptions of MINIVER and TPSX items were provided earlier. TCAT, the Thermal Calculation Analysis Tool, is currently under development by the author. It will use finite difference methods coupled with MDO methodology to correctly size the desired TPS materials for an RLV based on input from TPSX and MINIVER.

The numerical optimizer chosen will have the ability to use algorithms that can solve constrained and unconstrained design problems. Some of the constrained optimization algorithms will include modified method of feasible directions (MMFD), sequential linear programming (SLP), and sequential quadratic programming (SQP).

The diagram in Figure 3 gives a pictorial representation of the dynamic on-line TPS sizing

process. First, a “thinned” trajectory data from POST, an output file reduced to 50 points or less, is fed into MINIVER where a 2-D aeroheating analysis is conducted. This produces convective heating rates, heat loads and radiation equilibrium temperatures, which are calculated using empirical methods such as the Fay-Riddell stagnation point method and the Eckert’s reference enthalpy method for flat plate heating. The next step is to input a convective heat rate vs. time array and a material properties list into TCAT. In turn, TCAT and the optimizer will numerically solve and optimize for the thickness, unit weight and acreage percentage values of the TPS at each selected body point of the vehicle. Specifically, the optimizer will minimize the unit weights (thickness) based on several constraints. These include a maximum surface temperature, a maximum back-face temperature, and a technology readiness level (TRL) constraint.

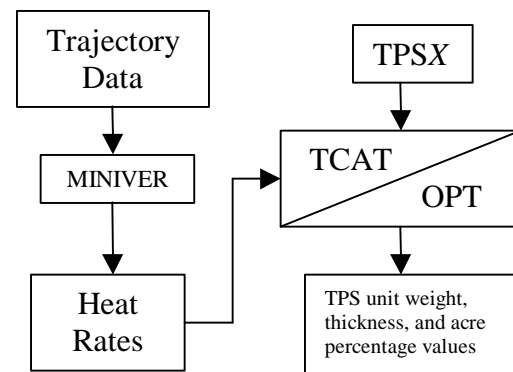


Figure 3. Dynamic on-line TPS sizing.

The temperature and heat rate on the surface of the vehicle decreases in the axial direction with the maximum at the stagnation point. This is due to the nature of a changing flow field over the body of the vehicle during ascent and reentry. As an example, the flow over the windward side of the vehicle is hotter and sees higher heating rates than the leeward side.

Once the point calculations are completed, aggregate values for the acre percentages for each TPS material used are calculated for the vehicle. Therefore, at each point where the analysis is conducted, there will be local values for the unit weight and thickness for the TPS material used. These

properties are then passed onto the Mass Properties discipline.

This process would normally be time consuming, but through scripting and automation of the data transfer, the manual work required by the user can be significantly reduced. This will make the process much faster. In summary, there are several advantages to having a dynamic on-line TPS sizing process. First of all, it will clearly provide a means of reaching near optimal values for the vehicle's TPS. Also, it will allow for a quicker turn around time for a TPS design as compared to the static off-line process. TCAT is a tool that will make dynamic TPS sizing possible.

TCAT

PURPOSE

TCAT is being developed for several reasons. First of all, it will provide a means to calculate the transient in-depth conduction seen by the surface of the TPS material that protects a vehicle during ascent and reentry. Along with the in-depth conduction, radiation from the surface of the material is calculated along with the temperature at the backface of the TPS material. Secondly, TCAT will give added speed and automation to the overall design process. Another driver in the development of TCAT is optimization. Also, TCAT will be well suited for use in a MDO environment by requiring minimal user input and assistance.

Table 1. % of Dry Wt of TPS for several vehicles.

Vehicle	% of Dry Wt.	Dry Weight (lbs)
Hyperion ³	6	123,250
Stargazer ⁴	14	34,750
Shuttle ⁵	16	154,739

In some vehicles, the TPS accounts for a high percentage of the overall vehicle dry weight (Table 1). This will lead to optimizing the weight of the TPS thereby lowering the percentage of the dry weight occupied by the TPS. Also, this will lower the cost of the TPS material and the cost of the vehicle.

METHODOLOGY

TCAT uses a fully implicit method in order to solve the one dimensional unsteady heat conduction equation (1) by marching in time

$$\frac{\partial T}{\partial t} = a \frac{\partial^2 T}{\partial x^2} \quad (1)$$

with the following boundary conditions,

$$q_{conv} - \epsilon \sigma T_s^4 + k \frac{dT}{dx} = 0 \quad \text{at } x = 0 \quad (2)$$

$$\frac{dT}{dx} = 0 \quad \text{at } x = L \quad (3)$$

$x = 0$ is at the top surface and $x = L$ is at the back-face. Equation (2) is an energy balance for the top surface of the TPS material that includes convection from the flow field, radiation from the heated surface, and conduction absorbed by the TPS material. Equation (3) states that there is an adiabatic wall at the back-face of the material. This assumption is used in order to model a semi-infinite heat sink.

Once the heat equation is discretized, a tridiagonal system of nonlinear equations results. This system is nonlinear due to the nonlinearity of equation (2) above. This system of equations is iteratively solved using the Newton-Raphson method at each time level. This is done at each time step over the whole trajectory. It is assumed that no kinetic reactions occur in the boundary layer; therefore, chemical equilibrium exists, but thermal equilibrium does not. Additionally, all material properties are held constant throughout all calculations.

TCAT can analyze up to 100 nodes in a single material, or 100 nodes total when several different TPS materials are layered together. The accuracy of the discretization for the surface and interface nodes is second order in space and first order in time. All interior nodes are first order accurate in space and time.

DEVELOPMENT

To date, three case studies have been developed and studied. Along with this, an analysis of several

dissimilar TPS materials layered together has also been conducted. The first case analyzes a single RCC tile in a vacuum. The top surface of the tile has the same boundary condition as equation (2). The bottom surface of the tile has the boundary condition seen in equation (4) accounts for conduction and radiation.

$$-k \frac{dT}{dx} - \epsilon \sigma T_s^4 = 0 \quad (4)$$

The second case looks at a one-meter nose radius 37° half-angle spherical cone (Figure 4) covered with UHTC flying straight and level at an altitude of 30.5 km at Mach 15. These cases are related because they demonstrate the computational methodology chosen can achieve steady state.

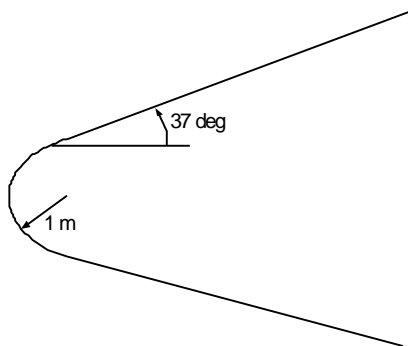


Figure 4. One-meter nose radius 37° half-angle spherical cone.

The third case is a transient analysis. It looks at the results of the cone shown in Figure 4 covered with RCC, and flown along the STS-1 reentry trajectory.⁶ Also, a transient analysis of several disparate TPS materials layered together was considered. It is important to have the transient analysis capability because it shows the effects of a time varying heat rate on the design of the TPS.

RESULTS

CASE 1: TILE IN A VACUUM

In this case, a 0.1016 m (4 in) thick RCC tile in a vacuum with a constant 200,000 W/m² convective heat rate applied to the surface of the material was analyzed. The boundary conditions on the top surface

of the tile are the same as in equation (2), while the back surface experiences radiation and conduction as given by equation (4). Table 2 shows the remainder of the assumptions used in this case.

Table 2. Case 1 Assumptions

Material	RCC
Density	1580 kg/m ³
Specific Heat	0.77 kJ/kg-K
Thermal Conductivity	4.3 W/m-K
Time Step	1 sec
Number of Nodes	10

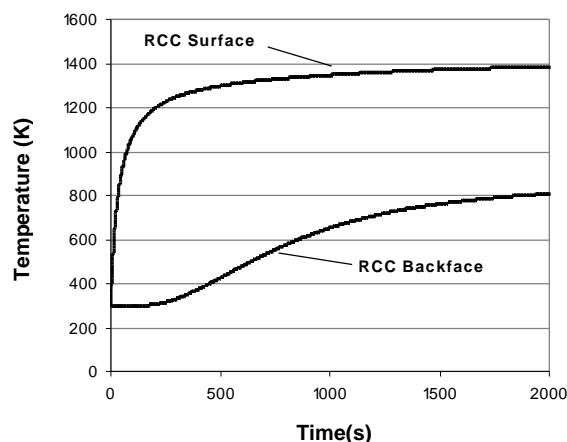


Figure 5. Temperature History.

Figure 5 shows the temperature history profile for the RCC tile in a vacuum. It can be seen that both the surface and back-face temperatures reach steady-state conditions. Both attain steady state at approximately 1400K and 800K respectively. These are both under the 1900 K multiuse temperature limit of RCC obtained from the TPSX database.

Figure 6 shows that all modes of heat transfer attain steady-state. As expected, the conduction started off equal to the value of the constant convection term and dropped off as the radiation on the surface increased. Also, it can be seen that the steady-state value radiation from the back-face lags and is small relative to that on the top surface, which is approximately 175,000 W/m². This is due to the fact that most of the convective heat is radiated away from the top surface, and it can be seen that the conduction and radiation at the backsurface reach an approximate steady-state value of 25,000 W/m².

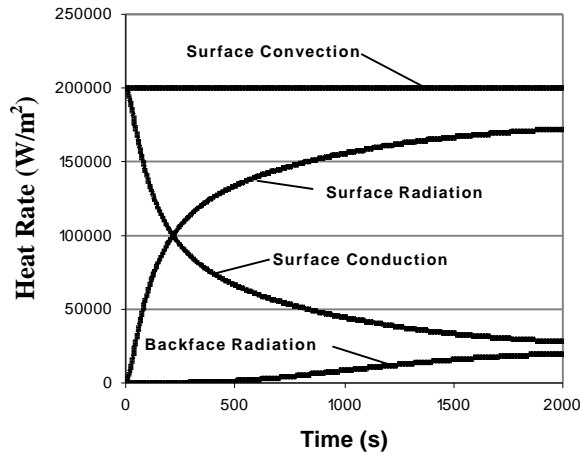


Figure 6. Heat Rate History.

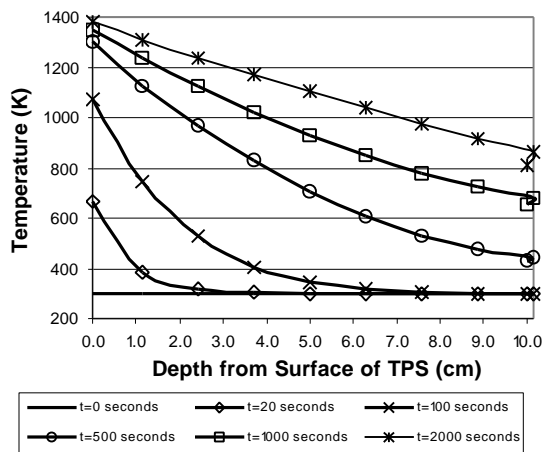


Figure 7. Internal Temperature Distribution.

Figure 7 shows the internal temperature distribution within the tile over the time span of 2,000 sec. As expected the temperature starts from the initial condition of 300 K and rises until steady state conditions exist within the material.

CASE 2: STRAIGHT AND LEVEL FLIGHT

In this case, the spherical-cone shown in Figure 4 was covered with 2.54 cm of UHTC flying straight and level at an altitude of 30.5 km at Mach 15. A model of the spherical cone was analyzed using MINIVER in order to attain the steady-state convective heat rates at each body point. The cone was flown at zero degrees angle of attack. For that reason, only results for one side of the cone will be

presented. Table 3 shows the assumptions that were used for this case.

Table 3. Case 2 Assumptions

Material	UHTC
Density	9520 kg/m ³
Specific Heat	0.27 kJ/kg-K
Thermal Conductivity	0.77 W/m-K
Time Step	1 sec
Number of Nodes	5

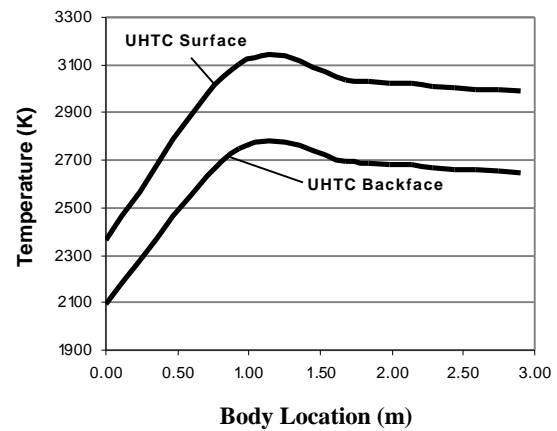


Figure 8. Steady-State Temperature Profiles.

In Figure 8, it is seen that the steady-state values of the temperatures on the top and back-face surfaces reach approximately 3000 K and 2700 K, respectively, and the maximum single-use temperature limit for UHTC is 3090 K. It is interesting to point out that maximum temperatures were not attained at the stagnation point, but at a location further downstream. This is due to the fact that the flow transitions from laminar to turbulent at a location behind the nose of the cone.

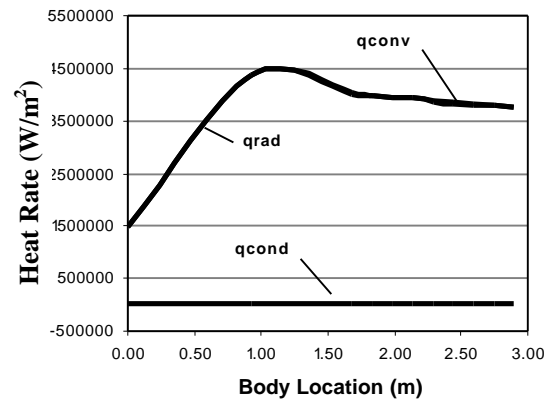


Figure 9. Steady-State Heat Rates.

Figure 9 shows the steady-state heat rate values for the different modes of heat transfer. As expected, the UHTC material radiated most of the heat away thereby reducing the amount of heat conducted into the material by two orders of magnitude. This occurs because the thermal conductivity of the UHTC material is high. Therefore, UHTC acts in the same manner of a conductor much like brass, which also has a high thermal conductivity. This mannerism is also accompanied by a high emissivity. Therefore, as the surface temperature rises, the amount of energy radiated away from the surface increases by a magnitude of 4 given by (2). This gives rise to the fact that over time most of convective heat into the material will be radiated away.

CASE 3: TRAJECTORY-BASED TRANSIENT ANALYSIS

The spherical-cone shown in Figure 4 was covered with RCC tiles and flown along the STS-1 descent trajectory. This was conducted in order to provide a proof of concept for a trajectory-based transient analysis capability. Table 4 lists the assumptions used in this analysis.

Table 4. Case 3 Assumptions

Material	RCC
Density	1580 kg/m ³
Specific Heat	0.77 kJ/kg-K
Thermal Conductivity	4.3 W/m-K
Time Step	1 sec
Number of Nodes	5

Figures 10-15 show temperature and heat rate histories for three points on the body of the spherical cone that was flown along the STS-1 descent trajectory. The first point is in the stagnation region of the cone, $S = 0$; the second lies on the windward side, $S = 0.925$ m; and the third point is on the leeward side of the cone, $S = 0.925$ m. ‘S’ corresponds to running length along the cone starting from the stagnation point.

In Figure 10, it can be seen that the maximum temperatures in the stagnation region were approximately 1600 K and 700 K on the surface and back-face, respectively. According to the TPSX database, these temperatures are clearly below the 1900 K multiple use limit of RCC. It is also clear

from this figure that the surface temperature peaked before that on the back surface. This demonstrates RCC’s ability to act an insulator.

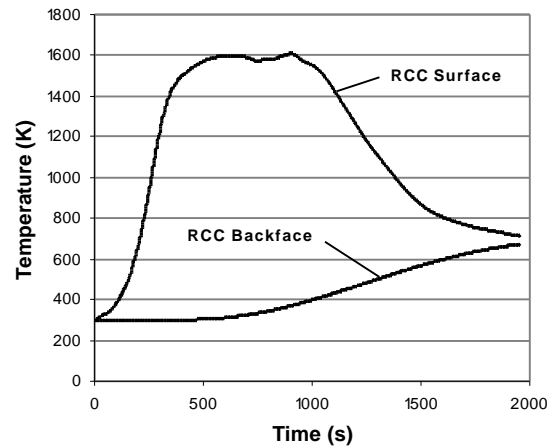


Figure 10. Stagnation Point Temperature History.

If the thickness of the RCC tile is increased, then the backface temperature will peak at a lower value than the one shown in Figure 10. The opposite would occur if the thickness of the RCC was decreased.

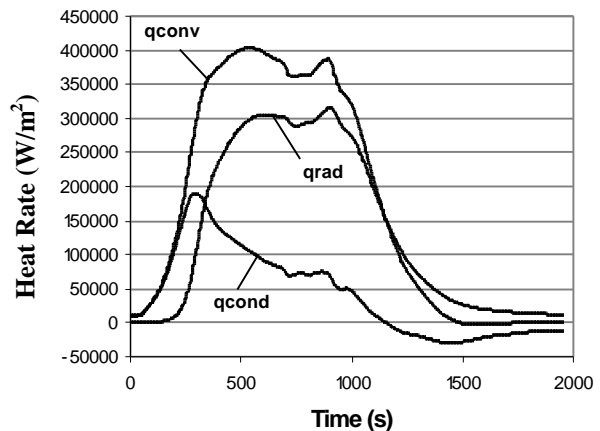


Figure 11. Stagnation Point Heating History.

The surface heat rate histories for the stagnation region of the 37° half-angle cone is shown above in Figure 11. The conductive heating rate follows the convective heating rate until the surface becomes hot enough to effectively radiate heat off the surface. This causes a slope change in the conductive heating rate. Eventually, the conductive heating rate becomes negative at the point where the radiative heat rate away from the surface of the RCC becomes greater than that of the convective heating rate. This means

that the flow field has become cooler than the surface of the material and heat is therefore being removed from the RCC material.

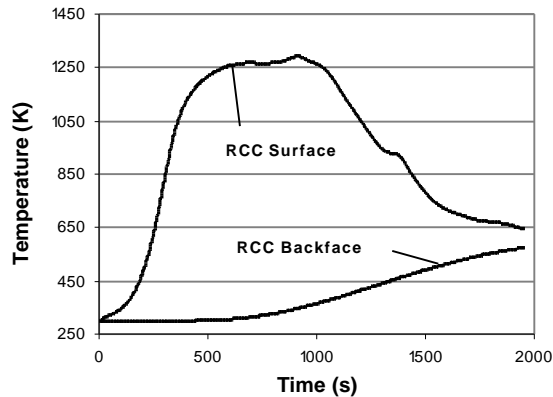


Figure 12. Windward Body Point Temp History.

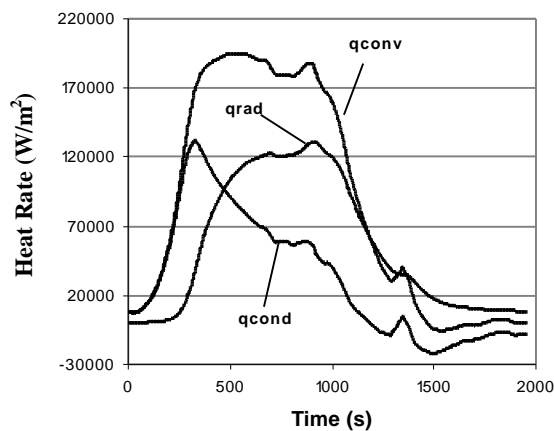


Figure 13. Windward Body Point Heating History.

Figures 12 and 13 above show the temperature and surface heating histories for the point located on the windward side of the vehicle at a running length of $S = 0.925$ m. The maximum temperature attained at this point is approximately 1300 K, which is less than the maximum temperature for the stagnation region. Also, the surface heat rate values for all modes of heat transfer were less than those at the stagnation region. This means that there is less of a heat load at this point, which leads to lower back-face temperatures over the course of the trajectory. This occurs because the integrated heat load at the windward side location is less than that at the stagnation point where the TPS material thickness is the same in both locations. Therefore, the thickness of the RCC tile could be

decreased because the TPS is overdesigned at this point on the body. If this were an actual vehicle design, the overdesign of the TPS would result in unnecessary TPS weight and higher overall cost associated with the vehicle.

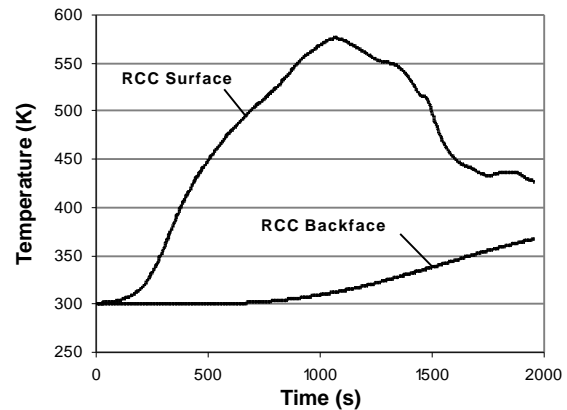


Figure 14. Leeward Body Point Temp History.

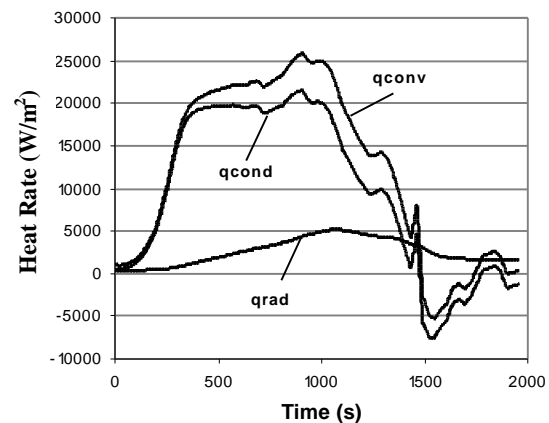


Figure 15. Leeward Body Point Heating History.

Figures 14 and 15 show the temperature and surface heating rate histories at a point on the leeward side of the spherical-cone analyzed. It is evident that the same trends are found here as at the stagnation region and windward side body points discussed earlier. Also, the temperature and surface heat rate values are lower than the other two body points because it located on the leeward side of the spherical-cone. On the leeward side, shocks are weaker when positive angles of attack are sustained, as is the case with the STS-1 decent trajectory.

Figure 16 gives a comparison of the temperature histories at each of the three points considered, and

reinforces the fact that the stagnation region has greater temperature values than the others considered.

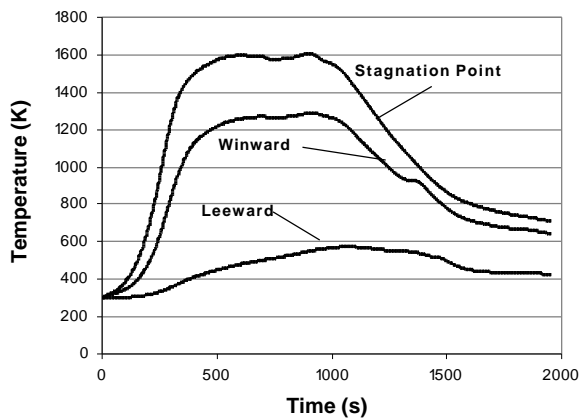


Figure 16. Temperature History Comparison.

STACK CAPABILITY

One of the most important attributes of TCAT is its ability to analyze several different TPS materials sandwiched together as a stack. A range of two to five TPS materials layered together can be analyzed at a time. Figure 17 shows a schematic of a five layer TPS stack, which is similar to that of the tiles on the Shuttle Orbiter.⁷

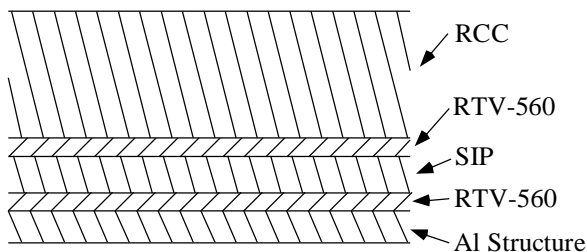


Figure 17. Schematic of TPS Stack.

The surface convective heat vs. time array obtained from the STS-1 trajectory analyzed in MINIVER was applied to the stack shown above. Table 5 shows the thickness and number of nodes used for each of the materials analyzed. Material properties were obtained from the NASA Ames TPSX database.

Numerically simulated temperature profiles for the surface, RCC/RTV interface and Al-Structure backface are shown in Figure 18. The figure shows that the stack served its purpose of thermally

insulating the aluminum structure from the severe flow field seen by the surface of the RCC. The temperature of the structure remained almost constant at 300 K while the surface attained a maximum of approximately 1600 K.

Table 5. Material Thickness and Number of Nodes.

Material	Thickness (mm)	No. of Nodes
RCC	152.4	10
RTV	2	3
SIP	4	3
RTV	2	3
Al-Structure	25.4	5

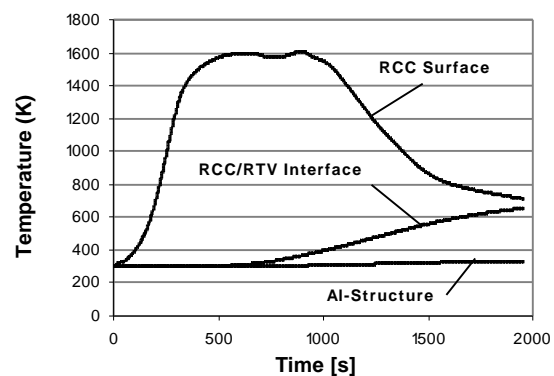


Figure 18: Temperature Distribution for TPS Stack of Five Materials.

BENCHMARKING TCAT

SINDA/G⁸ was the program used in order to benchmark the solutions obtained from TCAT. SINDA/G is a commercial thermal analysis tool created by Network Analysis Associates. It is capable of lumped parameter representations of physical problems governed by diffusion type equations. NASA Marshall provided the benchmark solutions through the use of this software package.

The results of the benchmark solutions are shown below. Figure 19 shows a comparison of the SINDA/G and TCAT results for the transient based analysis of RCC tiles on a 37° half-angle cone flown along the STS-1 reentry trajectory.

Also, the benchmark solution of the transient analysis of the TPS stack is shown in Figure 20. As can be seen, the SINDA/G and TCAT results match reasonably well. Therefore, this gives reassuring

confidence in the solution methodology used in TCAT. Also, benchmarking the solutions of TCAT provides a proof of concept for an analysis capability that will be integrated into a complex design loop for reusable launch vehicles.

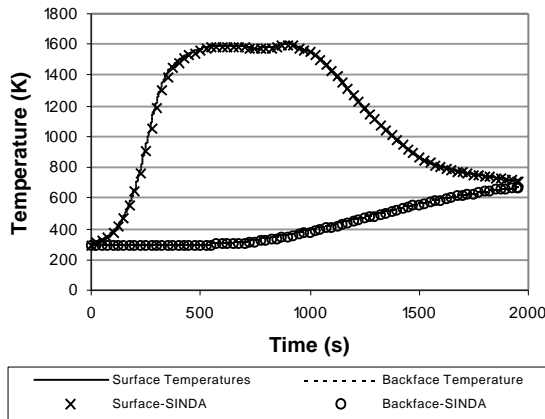


Figure 19. Benchmark Solution Comparison of TCAT for RCC tile on 37° half-angle cone.

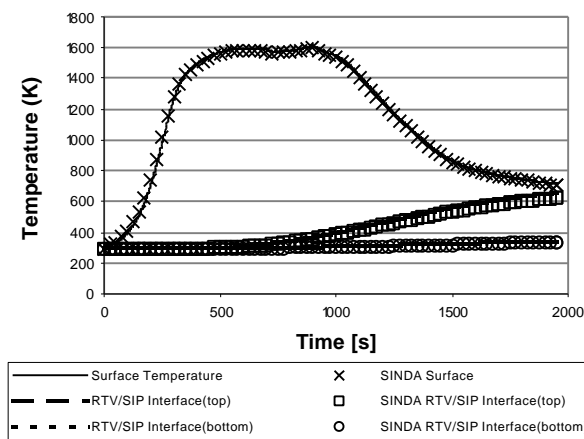


Figure 20. Benchmark Solution Comparison of TCAT for Five Material TPS Stack.

CONCLUSIONS

The purpose, methodology and development of a new tool that will provide the capability of incorporating Aeroheating and TPS sizing into a Design Structure Matrix was presented. Also, the process of dynamic TPS Sizing was presented. It was explained that a given trajectory from POST is thinned to 50 points. Once this is completed, MINIVER is used to conduct a two-dimensional aeroheating analysis over simplified body shapes. From MINIVER, a convective heat rate vs. time array is

input into TCAT along with a material properties list of the TPS stack. As mentioned, the TPS materials are obtained from the NASA Ames TPSX database. Using this process, the results of steady-state and transient analyses of different TPS materials and configuration were presented. Lastly, it was shown that the solutions obtained from TCAT matched very well with the benchmark results obtain from SINDA/G.

FUTURE WORK

Future work will consist of incorporating temperature dependent material properties into TCAT, coupling TCAT to an optimizer, and creating a web interface. Temperature dependent material properties will provide more accuracy in the solutions obtained from TCAT. The optimizer will allow the ability to minimize the weight of the overall TPS structure. This will be accomplished by minimizing the TPS material unit weights (thickness) subject to temperature and technology readiness level constraints. The web-interface will enable the TPS sizing process to be automated thereby reducing the overall TPS design time from hours to minutes. Not only will the web interface reduce the design time of the TPS sizing process, but it will also reduce the overall time required for designing the vehicle.

ACKNOWLEDGEMENTS

This research is funded under Cooperative Agreement NCC2-5332, with NASA Ames Research Center, and the United States Air Force Institute of Technology.

The authors would like to thank the members of the Georgia Institute of Technology Space System Design Laboratory (SSDL) and Reggie Alexander, Thermal analyst at NASA-MSFC, for their support.

REFERENCES

1. Engel, C.D. and Konishi, S., “MINIVER Upgrade for the AVID System”, NASA CR 172213, August 1993.

2. NASA Ames Thermal Protection Materials and System Branch, TPSX Database Internet Site: <http://asm.arc.nasa.gov>.
3. Olds, J., Ledsinger, L., "Stargazer: A TSTO Bantam-X Vehicle Concept Utilizing Rocket Based Combined-Cycle Propulsion," AIAA 99-4888, November 1999.
4. Olds, J.R., "Launch Vehicle Systems Analysis," NAG8-1302, January 1999.
5. Macconochie, I.O., and Klich, P.J., "Techniques For The Determination of Mass Properties of Earth-To-Orbit Transportation Systems," NASA TM 78661, June 1978.
6. Engel, C.D., and Schmitz, C.P., "Upgrade For the AVID System, VolumeII: LANMIN Input Guide," NAS1-17896, Remtech, Inc., Alabama, May 1987.
7. Norman, I., Rochelle, W.C, Kimbrough, B.S., "Comparison of Orbiter STS-2 Development Flight Instrumentation Data with Thermal Math Model Predictions," AIAA 82-0839, June 1982.
8. Behee, R., "Introduction to Thermal Modeling Using SINDA/G, A Tutorial Guide," Network Analysis Associates, Inc., California, 9th Edition, June 1994.